

<https://doi.org/10.70731/kgvvt42>

NADPH Oxidase 4 in Prostate Cancer: Expression and Potential Role in Ferroptosis

Kunlin He ^{a,†}, Jingxiao Li ^{a,†}, Gusheng Li ^a, Guanqiang Yan ^a, Xiang Gao ^a,
Huafu Zhou ^{a,*}, Jun Liu ^{a,*}

^a Department of Thoracic Surgery, The First Affiliated Hospital of Guangxi Medical University, Nanning, 530021, Guangxi Zhuang Autonomous Region, P. R. China

KEYWORDS

Prostate Cancer,
NOX4,
Ferroptosis,
Gene Expression,
Metabolic Pathways

ABSTRACT

Prostate cancer (PCa), the most common male malignant tumor worldwide, is associated with high morbidity and mortality, particularly when it progresses to metastatic disease. Ferroptosis, an iron-dependent form of cell death, has been implicated in various cancers. This study investigated the role of NADPH oxidase 4 (NOX4) in PCa and its potential connection to ferroptosis. By analyzing mRNA expression data from TCGA and GEO, NOX4 was found to be significantly upregulated in PCa tissues compared to non-cancerous tissues (SMD = 0.75, 95% CI: 0.41–1.10) and exhibited a moderate diagnostic accuracy (AUC = 0.79, 95% CI: 0.75–0.82). A total of 464 differentially co-expressed genes (DCEGs) were identified, including the hub genes BUB1, CCNB1, and CCNB2. Furthermore, NOX4 expression showed significant correlations with ferroptosis-related genes such as ALOX15, UBC, FTH1, and SLC2A6. Functional enrichment analyses (GO and KEGG) revealed that NOX4-associated DCEGs were enriched in metabolic pathways, cell cycle regulation, mitotic nuclear division, chromatin binding, and centromeric regions. These results suggest that NOX4 may contribute to ferroptosis regulation in PCa through its involvement in metabolic and cell cycle pathways, highlighting its potential as a therapeutic target.

1. Introduction

Prostate cancer (PCa) is the most common male malignant tumor in worldwide. According to *Cancer Statistics, 2025*, PCa accounted for 30% of all estimated new cases in men, which means over 313,780 new PCa cases in this year [1]. PCa in early stages is

less harmful to patients and the 15-year survival rate could reach 94% [2]. Current guidelines recommend surgery as the preferred treatment for PCa in early stages [3]. However, once the metastasis of tumor occurred, the 5-year survival rate of patients suffered PCa will reduce to 28% or less [4]. In recent years,

† These authors contributed equally to this work.

* Corresponding author. E-mail address: zhouhuafu_gxmu@163.com (Huafu Zhou), lj_gxmuyfy_c_t_s@163.com (Jun Liu)

androgen-targeted therapy (ADT) was widely used in metastatic PCa, but in the long-term follow-up process, some studies found that the low level of drug response and drug-induced apoptosis escape were still the main defects of ADT [5,6]. Therefore, finding new targets for molecular targeted therapy and proving the potential molecular mechanisms and signal pathways, then applying the new targets for diagnostic and treatment of PCa is vital.

Ferroptosis is an iron-dependent apoptosis pathway, which was considered to be related to neurodegeneration [7]. As a newly found apoptotic pathway, the groups of Galmiche and Louandre first reported the interaction mechanisms between ferroptosis and the anti-tumor drug sorafenib in hepatocellular carcinoma [8,9]. To date, ferroptosis had been pointed out related to the development of many cancers such as gastric cancer, head and neck cancer and liver cancer [10-12]. Moreover, some studies have indicated the relationship between ferroptosis and the development of PCa. Both Zhou and Tousignant reported that downregulation of GPX4 promotes ferroptosis in PCa cells, thereby inhibiting their proliferation and invasion [13,14]. When inducing PCa cells ferroptosis by drugs, Ghoochani et al. observed that some genes were differentially expressed in PCa cells with ferroptosis, which indicated the process of ferroptosis in PCa cells was probably related to differential expression of genes [15]. Nevertheless, existed researches had never clarified the relationship between the expression of transcription profile and ferroptosis in PCa cells and the research on the mechanisms of ferroptosis was still at a low stage.

NADPH oxidase 4 (NOX4), located in 11q14.3, acts not only in cellular energy metabolism but also as an electron donor to catalyze the electron transfer of molecular oxygen on the biofilm to produce reactive oxygen species (ROS) [16]. The growing evidence shows that NOX4 could be considered as an oncogene of PCa. Sampson et al. reported downregulated NOX4 was able to inhibit the activation of fibroblasts in prostate and block the process of tumorigenicity [17]. Wu et al. also indicated that low expressed NOX4 regulated by miRNA-137 influences glycolysis, cell proliferation and apoptosis in PCa, and NOX4 might be a potential target for PCa treatment [18]. Singh et al. observed that arsenic-induced overexpression of NOX4 promotes mitochondrial peroxidation in prostate epithelial cells, and then induces PCa [19]. However, it was a pity that despite numerous studies

on NOX4 in PCa, none had addressed the expression levels of NOX4 in PCa. In addition, the specific roles and potential mechanisms of ferroptosis regulated by NOX4 in PCa were still uncertain.

Thus, the present study aimed to explore the expression levels of NOX4 and potential mechanisms of NOX4-regulated ferroptosis in PCa. By detecting the mRNA expression levels of NOX4 and ferroptosis-related proteins in clinical samples and integrating with data from public databases, we aimed to reveal the relationship between the differentially expressed NOX4 and ferroptosis. Moreover, we herein estimated the correlation between NOX4 and tumor infiltrating immune cells in different tumor microenvironments based on Tumor Immune Estimation Resource (TIMER). Gene ontology (GO), Kyoto Encyclopedia of Genes and Genomes (KEGG) and Protein-protein interaction (PPI) networks analysis were applied to reveal signal pathways of NOX4 in ferroptosis process.

2. Method

2.1. The Clinical Significance of NOX4 in Pan-Cancer

2.1.1. The mRNA Expression Levels of NOX4 in Pan-Cancer

Tumor immune estimation resource, version 2 (TIMER 2.0) is a database including RNA-seq and tumor immune invasion data. In the present study, to explore the mRNA expression levels of NOX4 in pan-cancer, the authors entered NOX4 into TIMER 2.0. NOX4 expression data were observed for a total of 33 cancer types in TCGA, and box plot and independent sample t test were herein used to obtain the expression differences.

2.1.2. Prognostic Value of Differentially Expressed NOX4

Based on data from TCGA database, we extracted disease-free survival time of 12,357 patients from 33 cancer types. Univariate survival analysis was applied, and hazard ratios were performed to estimate the disease-free interval. By plotting the summary forest plot, the effect of differentially expressed NOX4 on the prognosis of patients with DFI could be observed directly.

2.2. The mRNA Expression Levels of NOX4 in PCa

2.2.1. MRNA Data Sources and Processing

Microarray and RNA-seq data for PCa were downloaded and screened from TCGA and Gene Express-

Table 1 | The included databases with NOX4 expression.

ID	Country	Platform	Year	Number of samples	
				PCa	Non-PCa
GSE26910	Italy	GPL570	2011	6	6
GSE32448	USA	GPL570	2011	40	40
GSE32982	Finland	GPL570	2011	6	3
GSE38043	USA	GPL570	2012	3	3
GSE46602	Denmark	GPL570	2013	34	14
GSE69223	Germany	GPL570	2015	15	15
GSE104749	China	GPL570	2017	4	4
GSE27616	USA	GPL4133	2011	9	4
GSE12378	UK	GPL5175	2008	36	3
GSE72220	USA	GPL5175	2015	57	90
GSE94767	UK	GPL5175	2017	185	33
GSE28204	China	GPL6480	2011	4	4
GSE35988	USA	GPL6480	2012	76	12
GSE32571	Germany	GPL6947	2011	59	39
GSE134073	Germany	GPL11154	2020	56	8
GSE60329	Italy	GPL14550	2014	108	28
GSE73397	China	GPL20952	2015	3	3
GSE88808	USA	GPL22571	2016	49	49
GSE134051	Germany	GPL26898	2020	216	39
TCGA+GTEx	NA	NA	NA	499	152

NOX4: NADPH oxidase 4; PCa: prostate cancer; TCGA: The Cancer Genome Atlas; GTEx: The Genotype-Tissue Expression.

sion Omnibus (GEO). A total of 22 datasets were collected using “prostate cancer” as the search keyword (Table 1). In order to make the results more objective, data from GEO and TCGA was subjected to $\log_2(x+1)$ conversion. Subsequently, the authors removed batch effects based on platforms, resulting in the selection of 11 studies.

2.2.2. Diagnostic Value of NOX4 in PCa

We performed a diagnostic test to assess the clinical significance of NOX4 in PCa. Based on expression levels of NOX4 in 11 studies, Stata 14.0 was used to estimate standard mean difference (SMD). If $P < 0.05$ or $I^2 > 50\%$, the study was considered to be heterogeneous, and a random-effect model would be applied. Otherwise a fixed-effects model was adopted. Receiver operating characteristic (ROC) curves of above studies were drawn by using IBM SPSS Statistics v23.0. Additionally, to evaluate the diagnostic potential of NOX4 comprehensively, a summary receiver operating characteristic (sROC) was plotted

through using Stata 14.0. The area under the curve (AUC) of sROC represents the diagnostic value of NOX4.

2.3. Obtention of NOX4 Differentially Co-Expressed Genes in PCa

2.3.1. Identification of NOX4 Co-Expressed Genes in PCa

Co-expressed genes (CEGs) were considered genes that had close relationship with NOX4 and were probably regulated by NOX4 in PCa. Gene expression from 11 studies was extracted. Through evaluating Pearson’s coefficient, we assessed the correlation between genes and NOX4. When $|r| > 0.3$ and $P < 0.05$, the gene would be considered one CEG. CEGs appeared more than five times in all 11 studies would be selected for subsequent research.

2.3.2. Identification of Differential Genes in PCa

After identifying CEGs of NOX4, we ran limma package to screen the differentially expressed genes (DEGs) of NOX4 in all GEO datasets, and we

Table 2 | The means and standard deviations of NOX4 expression values for PCa and non-PCa based on 11 studies.

Study	Sample type	PCa			Non-PCa		
		N	M	SD	N	M	SD
GPL570	Tissue	110	2.853	1.052	85	2.654	1.085
GPL4133	Tissue	9	2.354	0.870	4	0.199	1.182
GPL5175	Tissue	278	4.077	0.639	126	4.098	0.496
GPL6480	Tissue	80	2.123	1.350	16	0.647	1.067
GPL6947	Tissue	59	7.228	0.590	39	6.493	0.272
GPL11154	Tissue	56	7.953	1.525	8	6.153	0.870
GPL14550	Tissue	108	-0.073	1.342	28	-0.048	0.489
GPL20952	Tissue	3	9.627	0.239	3	9.575	0.070
GPL22571	Tissue	49	6.591	0.726	49	5.772	0.546
GPL26898	Tissue	216	6.430	0.616	39	5.952	0.340
TCGA+GTEx	Tissue	499	0.580	0.476	152	0.278	0.389

NOX4: NADPH oxidase 4; PCa: prostate cancer; N: number; M: mean; SD: standard deviation; TCGA: The Cancer Genome Atlas; GTEx: The Genotype-Tissue Expression.

screened DEGs in TCGA data with limma voom package. If the corrected $P < 0.05$ and $\log_2FC > 1$, the gene would be considered potential DEG. DEGs appeared more than five times in all 11 studies would be selected as NOX4 DEGs. Lastly, genes met in both two selection criteria would be identified as NOX4 DCEGs in PCa.

2.4. Obtention of Ferroptosis-Related Genes Regulated by NOX4 in PCa

FerrDB is a database focused on the research of genes that affect ferroptosis. Before performing the correlation analysis, we downloaded drivers, suppressors and markers of ferroptosis from ferrDB, and screened 219 genes using "Human only" as the screening criteria. Next, we intersected the above genes with NOX4 DCEGs, and ALOX15, UBC, FTH1 and SLC2A6 were identified as genes regulated by NOX4 in PCa. Correlation analysis was adopted to further explore the relationship between the expression levels of these genes.

2.5. Functional Enrichment Analysis of NOX4 DCEGs

In order to further explore the molecular mechanisms and potential functions of differentially expressed NOX4 regulated ferroptosis in PCa, we entered NOX4 DCEGs into Database for Annotation, Visualization, and Integrated Discovery (DAVID) v6.8. We herein chose GO and KEGG enrichment analysis to identify the molecular mechanisms and potential

functions of differentially expressed NOX4 regulated ferroptosis in PCa. GO terms and KEGG signaling pathways with $P < 0.05$ were identified. Moreover, PPI networks was constructed through Search Tool for the Retrieval of Interacting Genes (STRING) and Cytoscape v3.6.1. Hub genes of NOX4 DCEGs were identified based on the degree of nodes.

2.6. Immune-Related Analysis

We herein assessed the abundance of immune infiltrates in PCa tumor and paired paracancerous tissue through the correlation modules of TIMER 2.0. Besides, significantly correlated immune genes of NOX4 were also been assessed in Gene Expression Profiling Interactive Analysis (GEPIA). TISIDB integrates multiple heterogeneous datasets, which are able to predict interaction between tumor and immune system. In the present study, we observed the immune infiltration of NOX4 in a variety of tumors through TISIDB and showed the correlation between NOX4 and immune cells on scatter plots.

3. Results

3.1. The Clinical Significance of NOX4 in Pan-Cancer

The mRNA expression levels of NOX4 were analyzed in various cancer types based on TCGA. The results indicated that NOX4 was differentially expressed in many malignant tumors (Figure 1A).

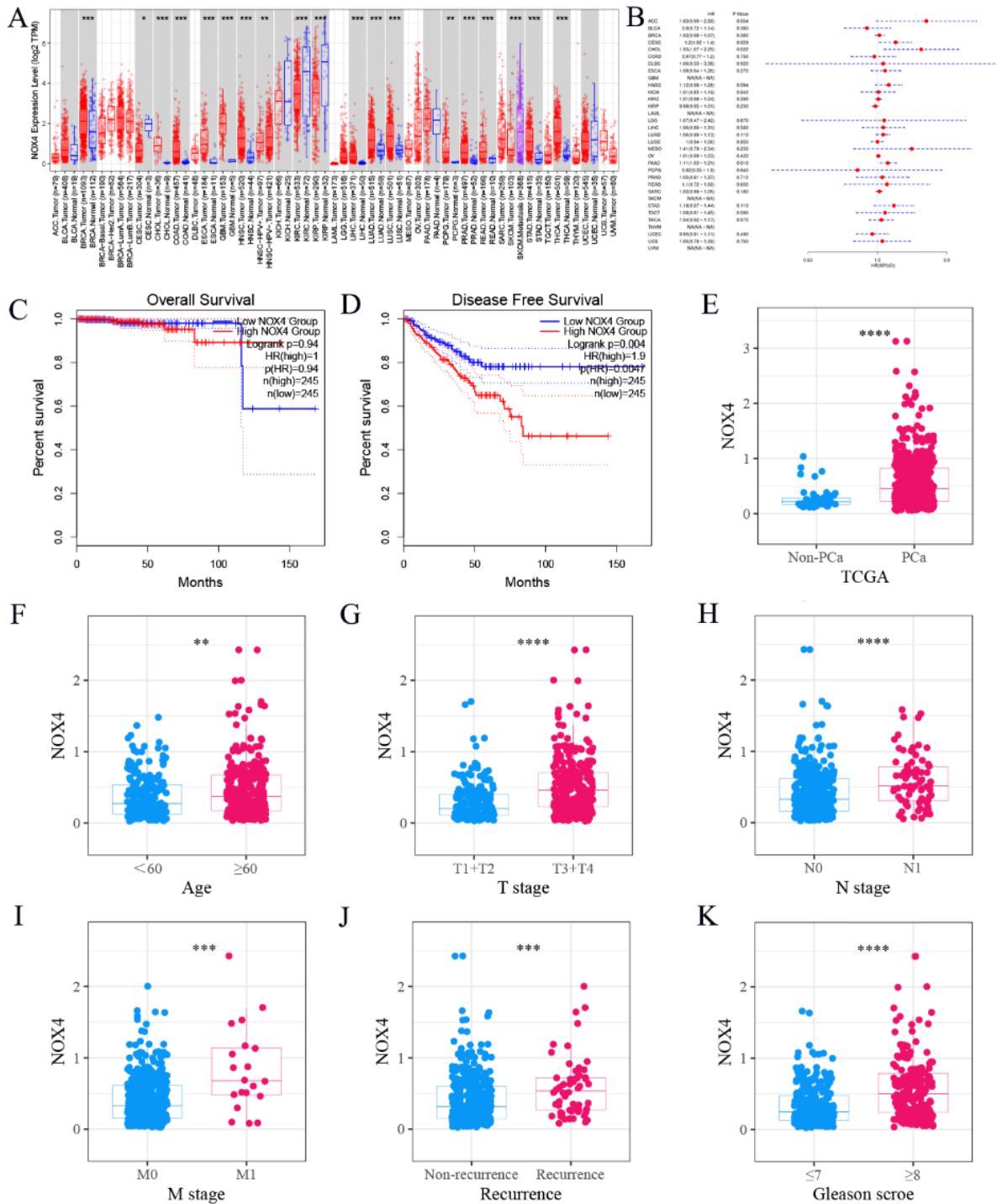


Figure 1 | (A) The mRNA expression levels of NOX4 in pan-cancer. (B) Disease-free intervals of patients with differentially expressed NOX4. (C,D) The OS and DFS between high and low expressed NOX4. (E-K) Expression of NOX4 in tissues of patients with different clinical parameters.

OS: overall survival. DFS: disease-free survival

Among these, NOX4 was upregulated in breast cancer, cholangiocarcinoma, colon adenocarcinoma, esophageal carcinoma, glioblastoma multiforme, head and neck squamous cell carcinoma, hepatocellular carcinoma, lung cancer, pheochromocytoma, paraganglioma, PCa, rectum adenocarcinoma,

Stomach adenocarcinoma and thyroid carcinoma. Conversely, NOX4 was downregulated in cervical cancer, kidney cancer. Additionally, disease-free interval of patients with differentially expressed NOX4 was shown on Figure 1B.

3.2. The mRNA Expression Levels and Diagnostic Value of NOX4 in PCa

In order to explore the mRNA expression of NOX4 in PCa, we extracted NOX4 expression data from 22 datasets from 11 platforms, including the TCGA and GEO database. The scatter plots comparing NOX4 expression between PCa and non-PCa tissues were shown in Figure 2. We used a random-effects model to calculate the standardized mean difference (SMD) for the included datasets, yielding significant heterogeneity ($I^2 = 88.3\%$, $P < 0.001$) and an SMD of 0.75 (95% CI: 0.41-1.10), which indicated that NOX4 was overexpressed in PCa (Figure 3A). However, no significant heterogeneity was detected (Figure 3B). Funnel plots revealed no publication bias (Figure 3C-E). Moreover, sROC showed that the AUC of NOX4 value was 0.79 (95%CI: 0.75-0.82), suggesting moderate sensitivity and specificity for PCa diagnosis (Figure 4). The overall survival (OS) and disease-free survival (DFS) were displayed on Figure 1C to D. To further investigate the clinical significance of differentially expressed NOX4 in PCa patients with different clinical parameters, independent sample t test was applied to estimate the NOX4 expression levels, and scope of the test included ages, TNM stages, recurrences and gleason scores of patients (Figure 1E-K).

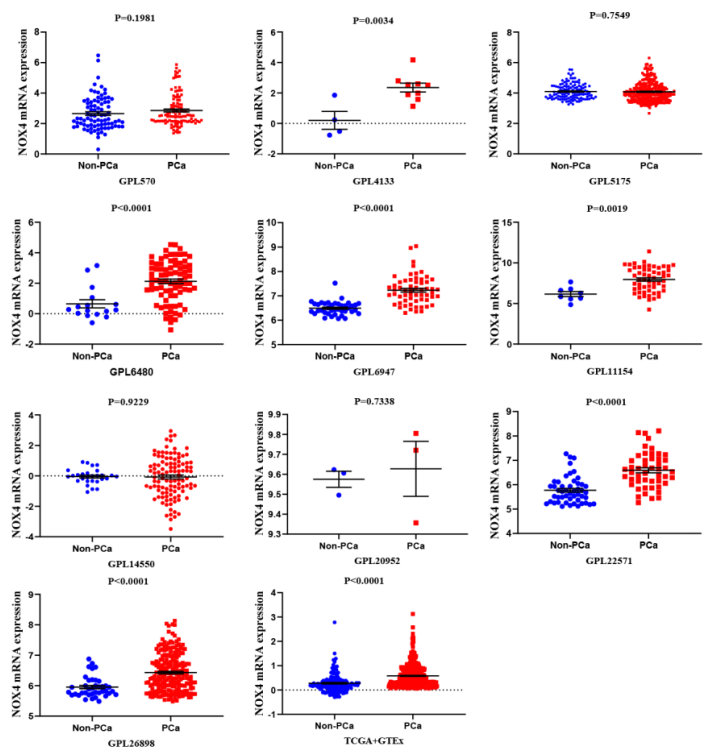


Figure 2 | The expression levels of NOX4 in 22 datasets from 11 platforms.

PCa: prostate cancer. TCGA: The Cancer Genome Atlas. GTEx: The Genotype-Tissue Expression project.

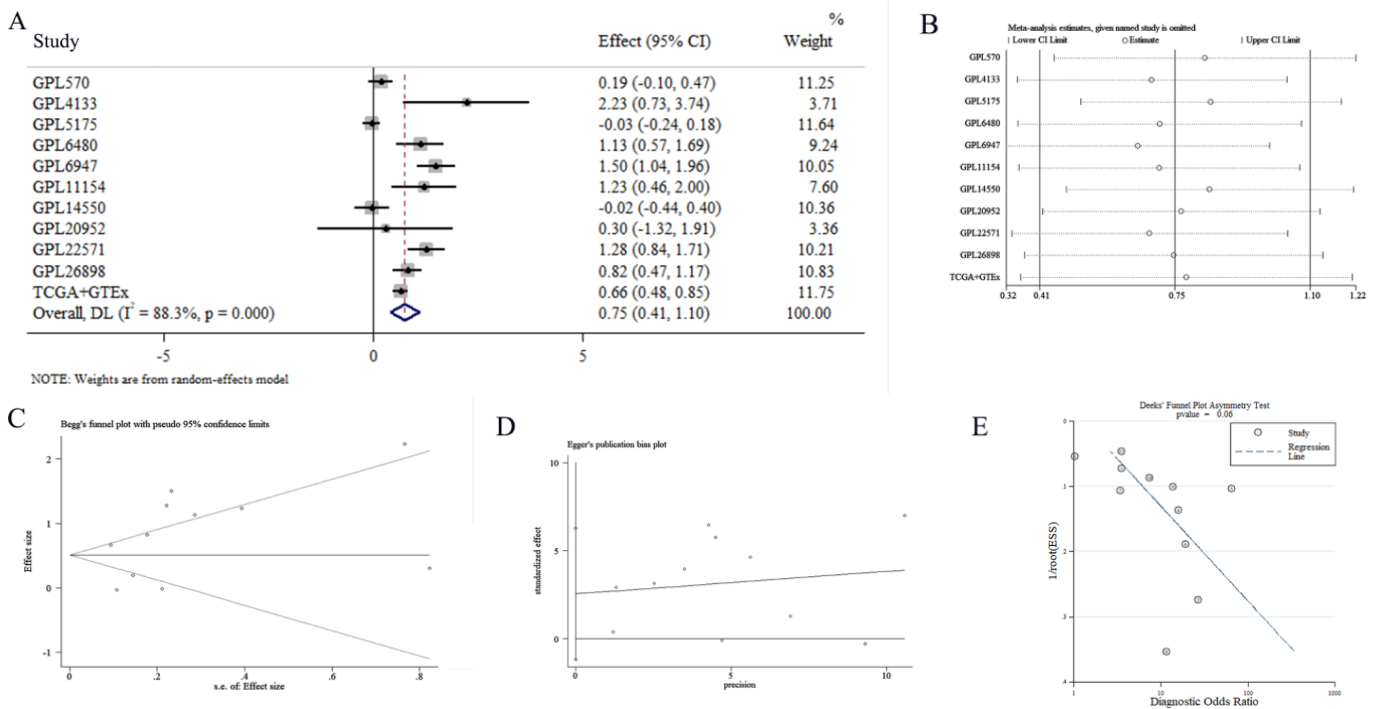


Figure 3 | The mRNA expression levels of NOX4 in PCa. (A) Forest plot showing a combined SMD of 0.75 (0.41 to 1.10), indicating that the expression of NOX4 in PCa is higher than that in non-PCa. (B) Sensitivity analysis showing the combined SMD is stable. (C, D, E) Begg's, Egger's and Deek's tests showing no publication bias ($p > 0.05$).

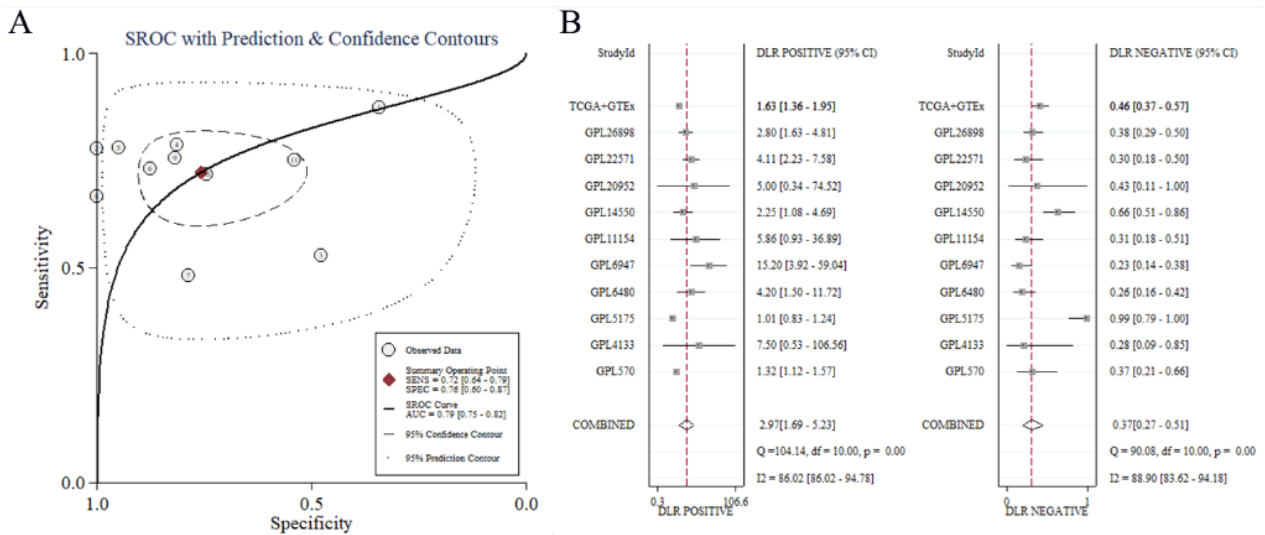


Figure4 | Discrimination potential of CELSR3 in PCa. (A) SROC curve assessing the discrimination potential of NOX4 in PCa. (B) Sensitivity and specificity analysis showed that NOX4 had a moderate predict potential in PCa.

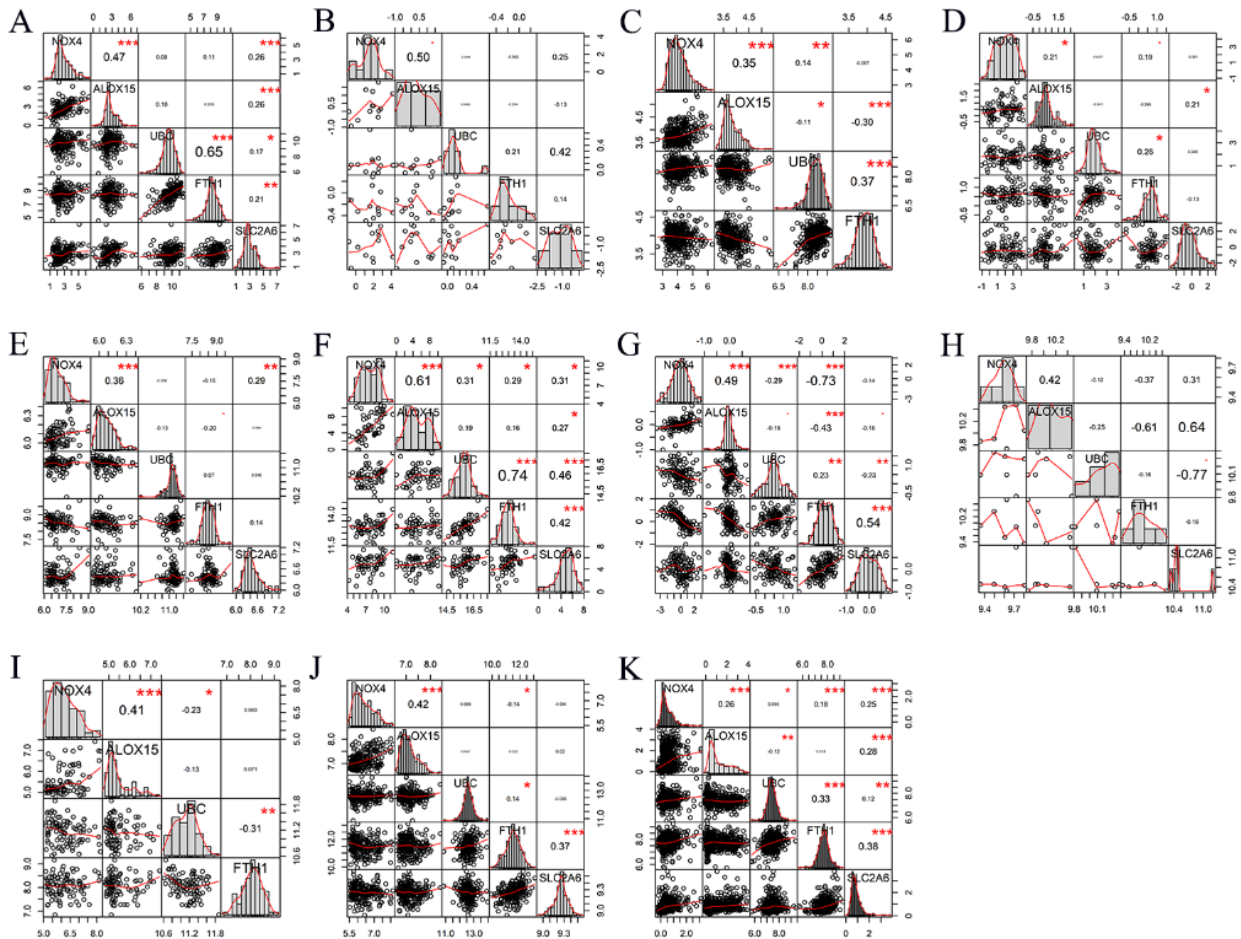


Figure5 | Correlation analysis showed that the expression of NOX4 had a considerable correlation with ferroptosis-related genes.

The pure number in bold represents Pearson correlation coefficient, and one or more “*” represent significant difference. (A-D) GPL570, GPL4133, GPL5175, GPL6480. (E-H) GPL6947, GPL11154, GPL14550, GPL20952. (I-K) GPL22571, GPL26898, TCGA+GTEX.

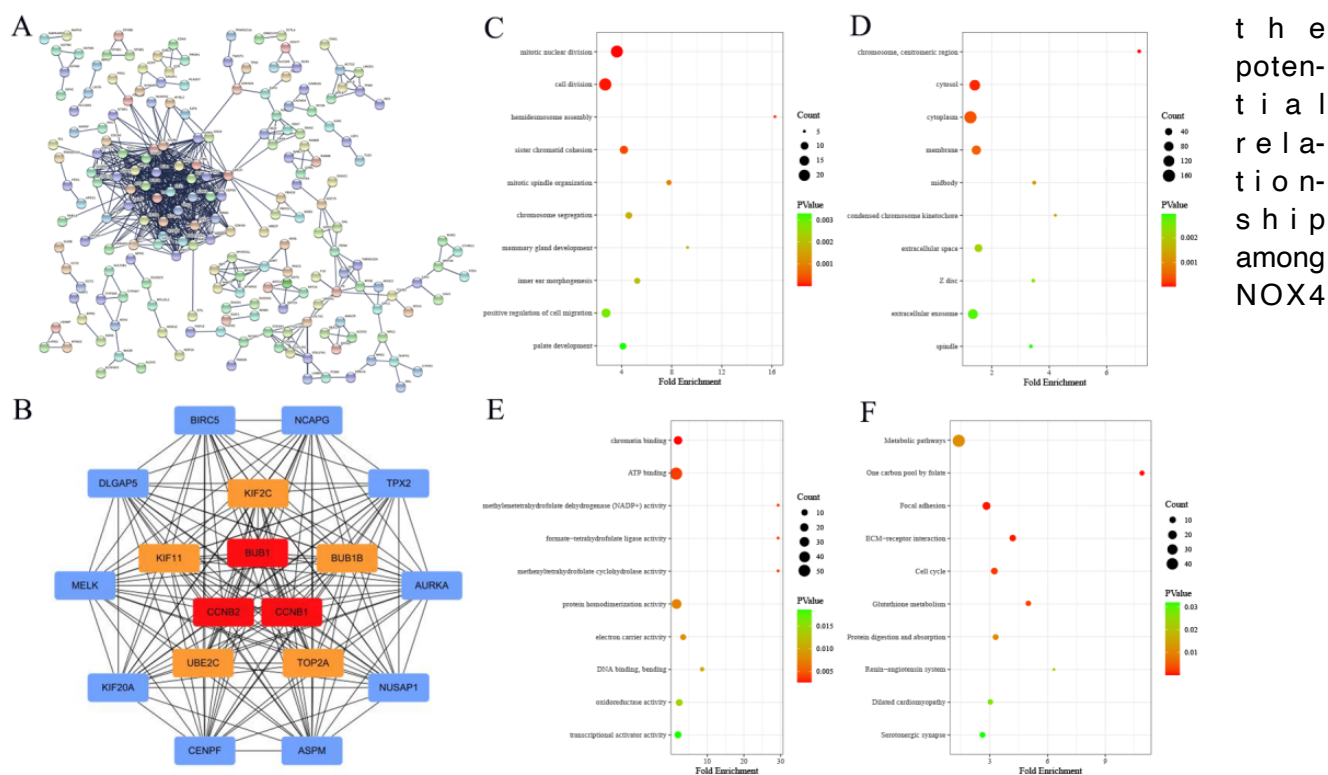


Figure 6 | Enrichment analysis

(A) PPI network analysis of NOX4 DCEGs. (B) BUB1, CCNB1, CCNB2 were identified as hub genes of NOX4. (C) Enrichment terms of NOX4 DCEGs in biological process. (D) Enrichment terms of NOX4 DCEGs in cellular component. (E) Enrichment terms of NOX4 DCEGs in molecular function. (F) Enrichment terms of NOX4 DCEGs in Kyoto Encyclopedia of Genes and Genomes.

3.3. Correlation Between NOX4 and Ferroptosis-Related Genes

We herein extracted mRNA expression data from 11 studies, and Pearson's coefficient analysis revealed that 945 CEGs were closely related to NOX4, including 685 positive related genes and 260 negative related genes. Differential expression analysis exhibited that 2663 DEGs were identified in PCa. A total of 464 genes were finally identified as NOX4 DCEGs in PCa. These 464 genes were used to intersect with genes from ferrDB, yielding 4 ferroptosis-related genes: ALOX15, UBC, FTH1 and SLC2A6, which were used for subsequent analysis. The correlation analysis was applied to assess the correlation between NOX4 and above 4 ferroptosis-related genes. The results showed that NOX4 had a considerable correlation with ferroptosis-related genes, indicating that NOX4 was probably related to ferroptosis (Figure 5).

3.4. Functional Enrichment Analysis of NOX4 DCEGs

To explore the molecular mechanisms and signal pathways, we used PPI network analysis to reveal

DCEGs. The PPI result was shown in Figure 6A. Next, we calculated the connection degrees of nodes and identified BUB1, CCNB1, and CCNB2 as hub genes of NOX4 (Figure 6B). Based on GO analysis, NOX4 DCEGs were significantly enriched in mitotic nuclear division, chromosome, centromeric region and chromatin binding (Figure 6C-E). According to KEGG analysis, the metabolic pathways were the most significantly enriched pathways among NOX4 DCEGs (Figure 6F).

3.5. Immune-Related Analysis

To investigate the relationship between NOX4 and immune infiltrating cells, we explored the correlations between NOX4 and immune marker sets of a variety of immune cells in PCa from TIMER 2.0 and GEPIA databases. The immune cells analyzed included different functional T cells, B cells, monocytes, TAMs, M1 and M2 macrophages, neutrophils, NK cells and DCs. We also adjusted the results for purity and found that NOX4 expression was significantly correlated with most of immune marker sets (Table 3). Additionally, we herein entered NOX4 into TISIDB and found that the expression levels of NOX4 were signif-

the potential relationship among NOX4

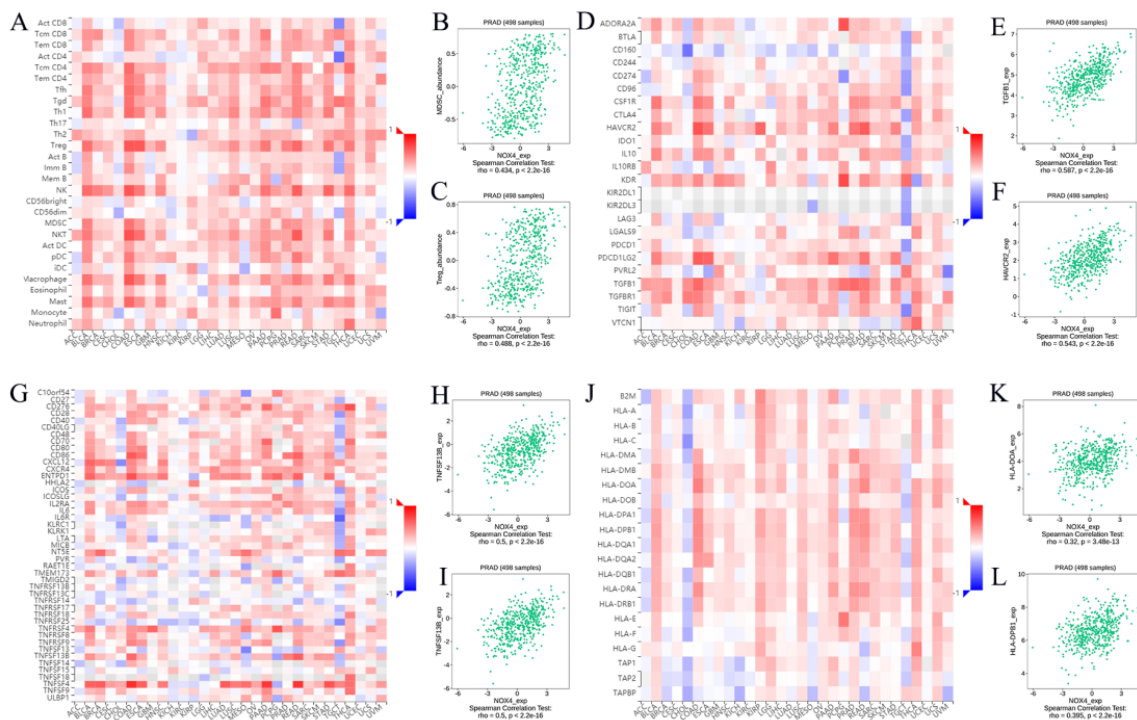


Figure 7 | (A,B,C) Associations of the NOX4 expression levels with lymphocytes, immunomodulators and chemokines in PCa. (D,E,F) Correlation analysis between the NOX4 expression levels and immunosuppressant. (G,H,I) The analysis results showed that NOX4 was related to immunoactivators. (J,K,L) Associations of the NOX4 expression levels with MHC molecules.

icantly correlated with lymphocytes, immunosuppressant, immunoactivators and MHC molecules in various cancer types. In this study, we displayed heat maps and scatter plots on Figure 7.

4. Discussion

NOX4 had been reported that correlated with ferroptosis of tumor cells in glioma and renal cell carcinoma [20,21]. The relationship between overexpressed NOX4 and the process of tumor cells development in PCa had also been covered [18]. However, there had no research indicated that the correlation between NOX4 and ferroptosis in PCa. The present study through analyzing the expression levels of NOX4 of PCa and paired paracancerous tissue samples from clinical collection and public databases, considered that upregulated NOX4 inhibit the development of PCa by regulating ferroptosis. Moreover, we performed an enrichment analysis to NOX4 DCEGs and considered metabolism pathway was probably a potential signal pathway for NOX4 to regulate ferroptosis. Immune infiltration analysis showed the expression levels of NOX4 was significantly related to various immune cells.

In previous studies, some scholars had mentioned the NOX4 expression levels in PCa. Low expression NOX4 was observed by Kim et al. in PCa cells treated with chalcone, and downregulated NOX4 inhibited the growth of tumor cells via ire1α-rid-miRNA-23b axis [22]. Harrison et al. also considered that NOX4 was overexpressed in PCa and had a positive correlation with metastasis [23]. Interestingly, Wu's group collected and analyzed the expression data of NOX4 from 65 clinical PCa samples. The results showed that downregulated NOX4 could increase the rate of apoptosis, which suggested that expressed NOX4 was a risk factor of PCa [18]. Through analyzing 20 paired epithelial tumor samples, Meitzler et al. reported that the overexpression frequency of NOX4 in PCa was only 36.8% [24]. To date, the expression levels of NOX4 in PCa had not been determined and the shortcomings of the existed research were also obvious, such as small sample sizes ($n < 65$) and most of them were single center studies. The present study collected and analyzed samples from clinical collection and public databases and reported the expression of NOX4 was upregulated in PCa for the first time based on a large sample size ($n = 2014$). Nevertheless, though we have obtained a larger sample

Table 3 | Correlation analysis between NOX4 markers of immune cells in PCa based on TIMER and GEPIA.-1

Gene marker	None		Purity		Tumour		Normal	
	Cor	P	Cor	P	Cor	P	Cor	P
CD19	0.141	**	0.108	*	0.14	**	0.39	**
CD20(KRT20)	0.192	***	0.167	***	0.057	0.21	0.093	0.51
CD38	-0.302	***	-0.352	***	-0.21	***	-0.21	0.13
CD8A	0.184	***	0.18	***	0.15	***	0.2	0.15
CD8B	0.126	**	0.131	**	0.26	***	0.2	0.16
BCL6	0.084	0.0635	0.05	0.308	0.017	0.71	0.18	0.19
ICOS	0.311	***	0.288	***	0.18	***	0.27	0.057
CXCR5	0.24	***	0.208	***	0.18	***	0.077	0.59
T-bet (TBX21)	0.284	***	0.278	***	0.23	***	0.29	*
STAT4	0.29	***	0.278	***	0.27	***	0.26	*
IL12RB2	0.233	***	0.247	***	0.17	***	0.073	0.61
WSX1(IL27RA)	0.254	***	0.243	***	0.24	***	0.25	0.078
STAT1	0.209	***	0.208	***	0.11	*	0.27	0.052
IFN-γ (IFNG)	0.215	***	0.167	***	0.14	**	0.24	0.089
TNF-α (TNF)	0.179	***	0.174	***	0.063	0.16	0.1	0.46
GATA3	0.095	*	0.047	0.344	-0.019	0.67	-0.22	0.12
CCR3	0.287	***	0.293	***	0.15	**	0.17	0.22
STAT6	-0.014	0.754	-0.023	0.638	-0.055	0.22	-0.019	0.89
STAT5A	0.221	***	0.213	***	0.2	***	0.11	0.44
TGFBR2	0.314	***	0.303	***	0.25	***	0.16	0.25
IRF4	0.315	***	0.308	***	0.092	*	0.37	**
PU.1(SPI1)	0.501	***	0.509	***	0.45	***	0.38	**
STAT3	0.176	***	0.165	***	0.057	0.21	0.27	0.053
IL-17A	0.027	0.543	0.005	0.927	-0.0022	0.96	0.06	0.67
CCR10	0.224	***	1.236	***	0.054	0.23	0.2	0.16
AHR	0.337	***	0.348	***	0.12	***	0.15	0.29
FOXP3	0.312	***	0.3	***	0.3	***	0.27	0.052
CD25(IL2RA)	0.499	***	0.485	***	0.4	***	0.48	***
CCR8	0.364	***	0.348	***	0.29	***	0.45	***
PD-1 (PDCD1)	0.236	***	0.243	***	0.26	***	0.42	**
CTLA4	0.357	***	0.352	***	0.48	***	0.37	**
LAG3	0.121	**	0.088	0.0736	0.11	*	-0.097	0.49
TIM-3 (HAVCR2)	0.57	***	0.572	***	0.53	***	0.34	*
CD68	0.524	***	0.514	***	0.38	***	0.37	**
CD11b (ITGAM)	0.448	***	0.454	***	0.34	***	0.35	**
INOS (NOS2)	0.044	0.324	0.001	0.981	-0.058	0.2	0.031	0.83
IRF5	0.526	***	0.525	***	0.36	***	-0.18	0.2
COX2(PTGS2)	0.061	0.178	0.043	0.385	-0.012	0.79	-0.13	0.38
ARG1	0.143	**	0.148	**	0.066	0.15	0.44	**
MRC1	0.428	***	0.44	***	0.29	***	0.29	*
MS4A4A	0.521	***	0.524	***	0.46	***	0.34	*
CCL2	0.264	***	0.247	***	0.054	0.23	0.23	0.096
CD80	0.444	***	0.417	***	0.42	***	0.24	0.091
CD86	0.553	***	0.571	***	0.43	***	0.35	*
CCR5	0.353	***	0.36	***	0.27	***	0.34	*
CD14	0.411	***	0.409	***	0.33	***	0.21	0.13
CD16(FCGR3B)	0.088	0.0489	0.082	0.0968	0.11	*	0.22	0.12
CD115 (CSF1R)	0.488	***	0.505	***	0.39	***	0.29	*
CD66b (CEACAM8)	0.001	0.978	-0.008	0.867	0.035	0.44	-0.04	0.78
CD15(FUT4)	0.043	0.338	0.023	0.639	0.037	0.41	-0.067	0.64
CD11b (ITGAM)	0.448	***	0.454	***	0.34	***	0.35	**
XCL1	0.144	**	0.128	**	0.16	***	0.17	0.23
CD7	0.187	***	0.194	***	0.19	***	0.35	*
KIR3DL1	0.112	*	0.104	0.0343	0.15	***	-0.071	0.91
CD1C(BDCA-1)	0.279	***	0.278	***	0.25	***	0.39	**
CD141(THBD)	0.239	***	0.228	***	0.14	**	0.026	0.86
CD11c (ITGAX)	0.513	***	0.501	***	0.39	***	0.35	*

size, long-term follow-up investigation and deeper research were essential if reliable conclusions were to be drawn.

In the process of discussing the prognosis of PCa patients, clinical parameters play a significant role. Based on TCGA database, we extracted the clinical parameters of PCa patients, including age, TNM stages, recurrence and gleason scores, and analyzed NOX4 expression levels in patients with different clinical parameters. The results were indicative of differentially expressed NOX4 existed in patients with diverse clinical parameters. NOX4 was expressed higher in patients with older ages, higher TNM stages, recurrence and higher gleason scores. To our knowledge, it was the first time to report NOX4 mRNA was differentially expressed in tissues of patients with diverse clinical parameters.

As a member of NADPH oxidases family, NOX4 mainly generates the ROS in astrocytes [25]. In the process of searching for literature, the authors found that NOX4 had been reported to be correlated with ferroptosis. Park et al. indicated the lipid peroxidation mediated by NOX4 in Alzheimer's disease was harmful to mitochondrion and promoted the accumulation of iron in astrocytes, resulting in the occurrence of ferroptosis [26]. Through knocking out NOX4 gene, Chen et al. observed that left ventricular remodeling occurred in rats and the incidence of ferroptosis in cardiomyocytes was reduced [27]. Yang et al. considered NOX4 was a hub gene of ROS-producing enzyme in renal cell carcinoma and the overexpressed NOX4 was a necessary condition of ferroptosis [21]. To date, the relationship between NOX4 and PCa cells ferroptosis had never been clarified. Based on the above results and the current researching gap, we decided to explore the correlation between the expression levels of NOX4 and ferroptosis-related proteins. We herein screened 4 ferroptosis-related genes and performed a correlation analysis with NOX4. The obtained results suggested that NOX4 had a moderate correlation with ferroptosis-related proteins in 20 studies from 11 platforms, which indicated NOX4 was probably related with ferroptosis in PCa.

To further explore the potential molecular mechanisms and signal pathways of ferroptosis regulated by NOX4 in PCa, herein we entered NOX4 DCEGs into STRING and constructed a PPI network. According to the PPI network analysis, we screened 3 hub genes, including BUB1, CCNB1 and CCNB2. Among the 3 selected hub genes, CCNB1 had been reported to be correlated with ferroptosis. In the process of treating T-cell lymphoma with artesunate (ART), Ishikawa et

al. found ART induced tumor cell peroxidation by activating CCNB1, thereby causing cell cycle arrest and iron accumulation and inhibiting the proliferation of tumor cells [28]. Though the mentioned research did not directly indicate the relationship between NOX4 and CCNB1, according to the pathway of tumor cell cycle arrested by CCNB1, we could infer that NOX4 caused lipid peroxidation, which was one of the factors leading to ferroptosis of tumor cells. However, this was the only study of NOX4 hub genes in ferroptosis, and the potential mechanisms of the above 3 genes and NOX4 in ferroptosis remained to be further explored in vivo and in vitro experiments.

As stated above, NOX4 and its hub genes were reported correlated with ferroptosis in other cancer types, we also found the expression of NOX4 was related to ferroptosis-related proteins. So how does differentially expressed NOX4 induce ferroptosis in PCa? We tried to applied enrichment analysis to DCEGs of NOX4, and the KEGG results showed that NOX4 DCEGs were significantly enriched in metabolism pathway. We searched the literature immediately based on this results. But unfortunately, there was no report about NOX4 regulating ferroptosis in PCa through metabolism pathway. Nevertheless, we found some serviceable information. In a cell experiment managed by Yi et al. , LnCap cells exhibited different levels of lipid metabolism and incidence of ferroptosis with different phospholipid content, they considered the changes in phospholipid metabolism may be an important pathway of ferroptosis in PCa [29]. Another article indicated that the activation of PI3K-AKT-mTOR pathway was able to influence the lipid metabolism in PCa cells, thereby inhibiting the occurrence of ferroptosis [30]. Tousignant et al. reported that the increase of lipid content in PCa cells could lead to the increase of membrane fluidity and lipid peroxidation, resulting in ferroptosis [14]. Considering these findings, the authors believed that DCEGs of NOX4 regulated the process of PCa ferroptosis by participating in metabolism pathway.

However, this study had some limitations. First, significant heterogeneity was observed in the present research. Due to the lack of sample size and clinical information, we could not find out the source of heterogeneity yet. Therefore, a random-effect model was applied. A larger clinical cohort should be used to validate our results in the future. Second, all PCa samples were extracted from tissues. The value of NOX4 in PCa ferroptosis should be verified in body fluids of

PCa patients. Lastly, the function of NOX4 in PCa needs to be further explored in vivo and in vitro.

5. Conclusion

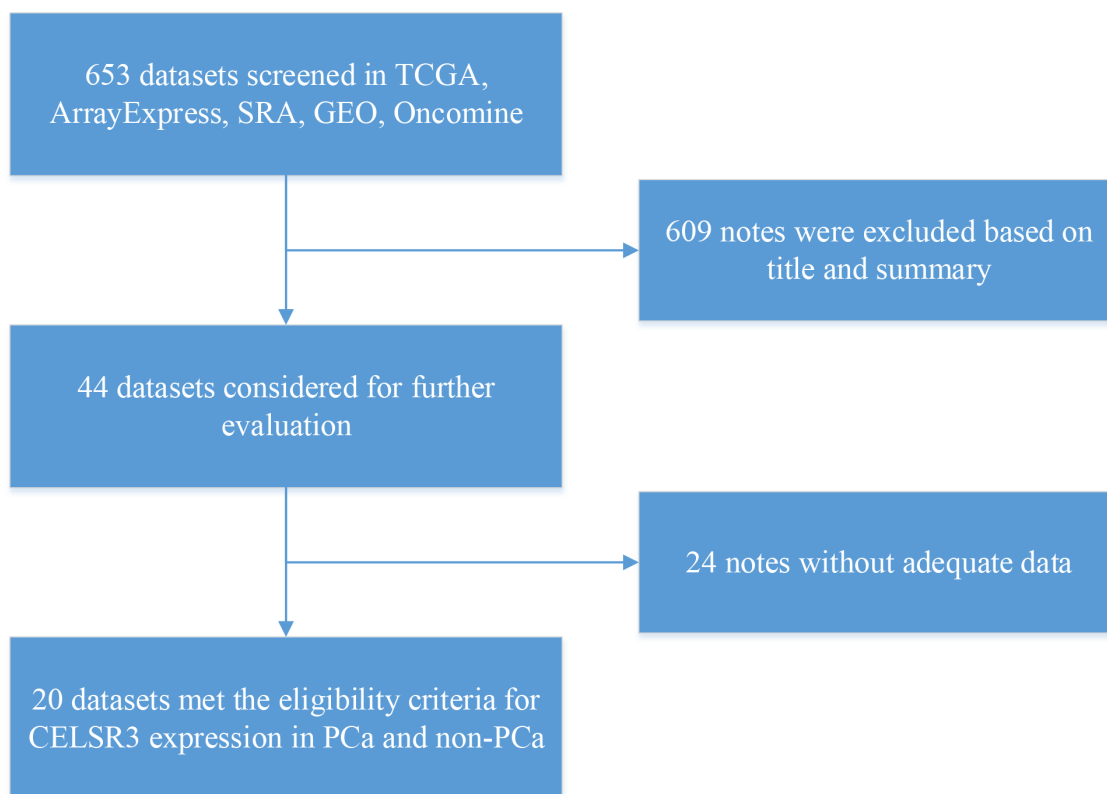
In summary, based on results from clinical samples and mRNA microarray and sequencing data from public databases, we herein concluded that NOX4 was downregulated in PCa and indicated the expression levels of NOX4 were correlated with ferroptosis-related proteins. Differentially expressed NOX4 might regulate the development of ferroptosis by participating in metabolism pathway, which needs to be verified in vivo and in vitro.

Reference

1. Siegel RL, Kratzer TB, Giaquinto AN, et al. Cancer statistics, 2025. *CA Cancer J Clin.* 2025 Jan-Feb;75(1):10-45.
2. Klotz L, Vesprini D, Sethukavalan P, et al. Long-term follow-up of a large active surveillance cohort of patients with prostate cancer[J]. *Journal of Clinical Oncology: Official Journal of the American Society of Clinical Oncology*, 2015, 33(3): 272-277.
3. Ahdoot M, Lebastchi A H, Turkbey B, et al. Contemporary treatments in prostate cancer focal therapy[J]. *Current Opinion in Oncology*, 2019, 31(3): 200-206.
4. Kelly S P, Anderson W F, Rosenberg P S, et al. Past, Current, and Future Incidence Rates and Burden of Metastatic Prostate Cancer in the United States[J]. *European Urology Focus*, 2018, 4(1): 121-127.
5. Harada K, Shiota M, Minato A, et al. Treatment Strategies for Metastatic Castration-Sensitive Prostate Cancer: From “All-Comers” to “Personalized” Approach[J]. *OncoTargets and Therapy*, 2021, 14: 2967-2974.
6. Crawford E D, Heidenreich A, Lawrentschuk N, et al. Androgen-targeted therapy in men with prostate cancer: evolving practice and future considerations[J]. *Prostate Cancer and Prostatic Diseases*, 2019, 22(1): 24-38.
7. Dixon S J, Lemberg K M, Lamprecht M R, et al. Ferroptosis: an iron-dependent form of nonapoptotic cell death[J]. *Cell*, 2012, 149(5): 1060-1072.
8. Louandre C, Ezzoukhry Z, Godin C, et al. Iron-dependent cell death of hepatocellular carcinoma cells exposed to sorafenib. *Int J Cancer.* 2013 Oct 1;133(7):1732-42.
9. Galmiche A, Chauffert B, Barbare J C. New biological perspectives for the improvement of the efficacy of sorafenib in hepatocellular carcinoma[J]. *Cancer Letters*, 2014, 346(2): 159-162.
10. Zhang H, Deng T, Liu R, et al. CAF secreted miR-522 suppresses ferroptosis and promotes acquired chemoresistance in gastric cancer. *Mol Cancer.* 2020 Feb 27;19(1):43.
11. Shin D, Kim EH, Lee J, et al. Nrf2 inhibition reverses resistance to GPX4 inhibitor-induced ferroptosis in head and neck cancer. *Free Radic Biol Med.* 2018 Dec;129:454-462.
12. Mao L, Zhao T, Song Y, et al. The emerging role of ferroptosis in non-cancer liver diseases: hype or increasing hope? *Cell Death Dis.* 2020 Jul 9;11(7):518.
13. Zhou X, Zou L, Chen W, et al. Flubendazole, FDA-approved anthelmintic, elicits valid antitumor effects by targeting P53 and promoting ferroptosis in castration-resistant prostate cancer[J]. *Pharmacological Research*, 2021, 164: 105305.
14. Tousignant K D, Rockstroh A, Poad B L J, et al. Therapy-induced lipid uptake and remodeling underpin ferroptosis hypersensitivity in prostate cancer[J]. *Cancer & Metabolism*, 2020, 8: 11.
15. Ghoochani A, Hsu E C, Aslan M, et al. Ferroptosis Inducers Are a Novel Therapeutic Approach for Advanced Prostate Cancer[J]. *Cancer Research*, 2021, 81(6): 1583-1594.
16. Lu JP, Monardo L, Bryskin I, et al. Androgens induce oxidative stress and radiation resistance in prostate cancer cells through NADPH oxidase. *Prostate Cancer Prostatic Dis.* 2010 Mar;13(1):39-46.
17. Sampson N, Brunner E, Weber A, et al. Inhibition of Nox4-dependent ROS signaling attenuates prostate fibroblast activation and abrogates stromal-mediated protumorigenic interactions. *Int J Cancer.* 2018 Jul 15;143(2):383-395.
18. Wu QQ, Zheng B, Weng GB, et al. Downregulated NOX4 underlies a novel inhibitory role of microRNA-137 in prostate cancer. *J Cell Biochem.* 2019 Jun;120(6):10215-10227.
19. Singh B, Kulawiec M, Owens KM, et al. Sustained Early Disruption of Mitochondrial Function Contributes to Arsenic-Induced Prostate Tumorigenesis. *Biochemistry (Mosc).* 2016 Oct;81(10):1089-1100.
20. Wang Z, Ding Y, Wang X, et al. Pseudolaric acid B triggers ferroptosis in glioma cells via activation of Nox4 and inhibition of xCT[J]. *Cancer Letters*, 2018, 428: 21-33.
21. Yang WH, Ding CC, Sun T, et al. The Hippo Pathway Effector TAZ Regulates Ferroptosis in Renal Cell Carcinoma. *Cell Rep.* 2019 Sep 3;28(10):2501-2508.e4.
22. Kim H K, Lee H Y, Riaz T A, et al. Chalcone suppresses tumor growth through NOX4-IRE1 α sulfonation-RIDD-miR-23b axis[J]. *Redox Biology*, 2021, 40: 101853.
23. Harrison I P, Vinh A, Johnson I R D, et al. NOX2 oxidase expressed in endosomes promotes cell proliferation and prostate tumour development[J]. *Oncotarget*, 2018, 9(83): 35378-35393.
24. Meitzler J L, Makhlof H R, Antony S, et al. Decoding NADPH oxidase 4 expression in human tumors[J]. *Redox Biology*, 2017, 13: 182-195.
25. Nayernia Z, Jaquet V, Krause KH. New insights on NOX enzymes in the central nervous system. *Antioxid Redox Signal.* 2014 Jun 10;20(17):2815-37.

26. Park M W, Cha H W, Kim J, et al. NOX4 promotes ferroptosis of astrocytes by oxidative stress-induced lipid peroxidation via the impairment of mitochondrial metabolism in Alzheimer's diseases[J]. Redox Biology, 2021, 41: 101947.
27. Chen X, Xu S, Zhao C, et al. Role of TLR4/NADPH oxidase 4 pathway in promoting cell death through autophagy and ferroptosis during heart failure[J]. Biochemical and Biophysical Research Communications, 2019, 516(1): 37-43.
28. Ishikawa C, Senba M, Mori N. Evaluation of artesunate for the treatment of adult T-cell leukemia/lymphoma[J]. European Journal of Pharmacology, 2020, 872: 172953.
29. Yi X, Li Y, Hu X, et al. Changes in phospholipid metabolism in exosomes of hormone-sensitive and hormone-resistant prostate cancer cells[J]. Journal of Cancer, 2021, 12(10): 2893-2902.
30. Yi J, Zhu J, Wu J, et al. Oncogenic activation of PI3K-AKT-mTOR signaling suppresses ferroptosis via SREBP-mediated lipogenesis[J]. Proceedings of the National Academy of Sciences of the United States of America, 2020, 117(49): 31189-31197.

Supplementary material 2 Datasets collection flowchart



Supplementary material 1 Research design flowchart

